Available online at www.sciencedirect.com

ScienceDirect

Mendeleev Commun., 2024, **34**, 442–445

Mendeleev Communications

Investigation of the carbon monoxide resistance of platinum catalysts prepared *via* pulse alternating current technique

Nikita A. Faddeev,* Alexandra B. Kuriganova, Igor N. Leontyev and Nina V. Smirnova

Platov South-Russian State Polytechnic University, 346428 Novocherkassk, Russian Federation.
E-mail: nikita.faddeev@yandex.ru

DOI: 10.1016/j.mencom.2024.04.042

The platinum catalysts based on carbon black and carbon nanotubes supports have been obtained *via* pulse alternating current technique. The synthesized Pt/C catalysts showed better electric transport characteristics and the carbon monoxide poisoning resistance in comparison with the commercial Pt/C owing to both the size of the platinum nanoparticles and their agglomeration on the support surface, and the morphology of the carbon support.

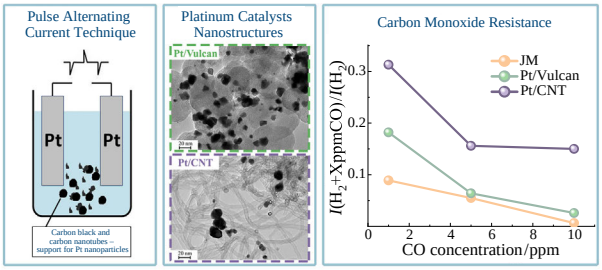

Keywords: platinum catalysts, pulse alternating current, fuel cells, carbon monoxide resistance, hydrogen.

Proton exchange membrane fuel cells (PEMFC) are highly efficient power sources. The main advantages of PEMFC are high power density, fast start-up time, low operating temperature and net zero carbon dioxide emissions.[1] They can contribute to meeting global energy demands while overcoming environmental challenges.[2] The most important issue facing PEMFC manufacturers and users is the durability of the PEMFC.[3] The stable operation of a single fuel cell, (membrane–electrode assembly) is determined by its components, *viz*. the membrane and catalyst.[4,5] But the purity of fuel (hydrogen) is especially important in PEMFC operation. Contaminants, such as hydrogen sulphide, ammonia and carbon monoxide (CO),[6] are known to be particularly pernicious and affect performance, even when they are present in trace (ppm) amounts.[7] Carbon monoxide is extremely harmful.

Today, half of the world hydrogen is produced by steam reforming of methane, natural gas or other hydrocarbons.[8] This process offers high conversion to hydrogen at low cost and high efficiency. Autothermal methane reforming and coal gasification are other proven and commercialized technologies.[9,10] Although these are the most devmature and economically viable technologies, the hydrogen produced is not suitable for direct use in PEMFC. The reformed product obtained after the first purification stage of the water–gas shift reaction – converted gas – possesses a typical composition: 40–70% H_2, 15–25% CO_2, 1–2% CO and small amounts of inert gases, *e.g.* methane, water vapor and nitrogen. The main mechanism to reduce PEMFC parameters in the presence of CO in the fuel is the poisoning of platinum-containing catalysts due to the irreversible adsorption of CO.[11] CO adsorption results in the reduction in the proportion of active sites on the platinum catalyst available for the target process, which affects the kinetics of electrocatalytic hydrogen oxidation. Methane and CO_2 are not so actively adsorbed on catalysts, but, being conditionally inert components, they can cause fuel starvation by reducing the hydrogen content of the fuel gas. In addition, a water shift reaction may occur with the formation of CO and its subsequent adsorption on platinum in the presence of water vapor.

The process of electrochemical oxidation of CO on platinum group metals has been extensively stdied.[12] CO-stripping is the most accurate method to determine the electrochemically active surface area of Pt-containing electrocatalysts. The electrochemical oxidation of CO on platinum occurs through the Langmuir–Hinshelwood mechanism. This involves the adsorption of CO and oxygen-containing particles on platinum, followed by their chemical interaction on the catalyst surface. It is important to note that CO irreversibly adsorbs on platinum over a wide range of potentials.

The resistance of the anodic catalyst to carbon monoxide poisoning is one of the most important properties of Pt/C electrocatalysts in PEMFC, toget well as its stability. Previously, we have demonstrated thnfluence of the preparation technique of the Pt/C catalyst and the morphology of the carbon support in the composition of such catalysts on their stability during long term cycling. Here, the study of carbon monoxide resistance of various platinum-based catalysts is discussed.

Platinum electrocatalysts were prepared by depositing Pt nanoparticles on the carbon support by electrochemical dispersion under the action of AC pulsed current, as described in details in our previous papers.[13–15] Carbon black Vulcan XC-72 (Cabot, S_{BET} = 37 m^2 g^{-1}) and multi-walled carbon nanotubes produced by the catalytic pyrolysis of methane on Fe–Mo/MgO (S_{BET} = 25 m^2 g^{-1}) were used as a support for platinum nanoparticles. The synthesized catalysts were referred as Pt/Vulcan and Pt/CNT. A commercial Pt/C catalyst (Johnson Matthey, referred as JM), was used for comparison.

The transmission electron microscopy (TEM) images [Figure 1(*a*),(*b*)] showed that platinum particles were uniformly distributed over the carbon black surface [Figure1(*a*),(*c*)]. However, the presence of agglomerates larger than 14 nm is more characteristic of the Pt/CNT catalyst [Figure 1(*b*),(*e*)]. According to TEM data, the average size of platinum nanoparticles (<*d*>) for catalysts produced *via* PAC technique is 3–5 times larger than the size of Pt nanoparticles of the commercial JM catalist (see Table 1).

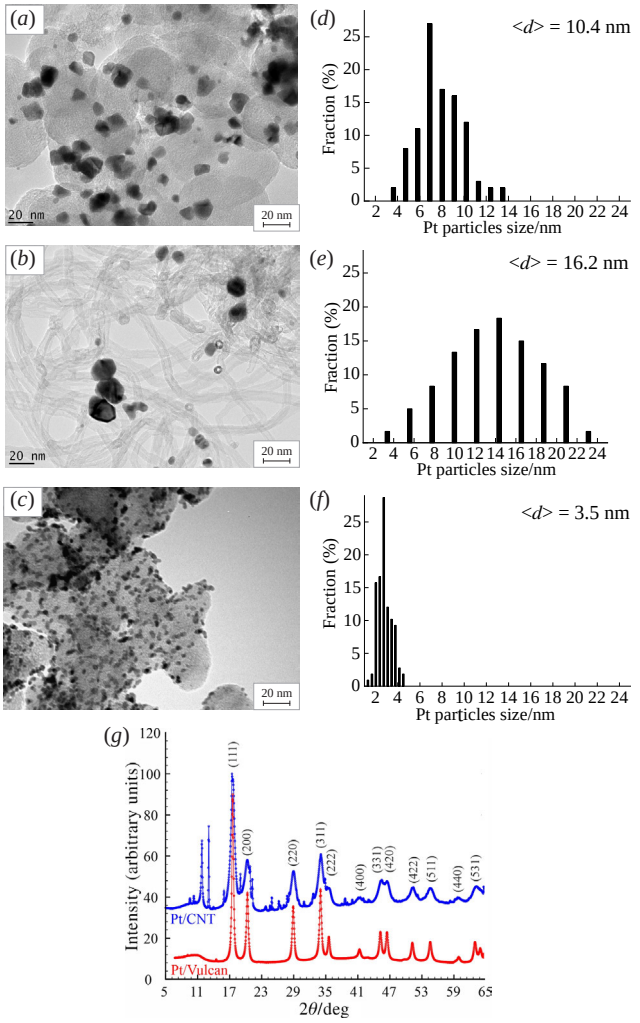

Figure 1 (*a*)–(*c*) TEM images and (*d*)–(*f*) histograms of platinum nanoparticle size distribution: (*a*) and (*d*) Pt/Vulcan, (*b*) and (*e*) Pt/CNT catalysts, obtained *via* PAC technique and (*c*) and (*f*) JM commercial catalyst; (*g*) XRD patterns of Pt/C catalysts.

The X-ray patterns of all synthesized Pt/C catalysts are shown in Figure 1(*g*). They indicate that all wide diffraction peaks of the XRD patterns corresponding to the reflections of face centered cubic (fcc) structure of platinum (Pt) can be assigned to JCPDS Card 04-0802. The average size of the nanoparticles and the unit cell parameters are determined by Rietveld refinement[16] (see Table 1). The powder diffraction pattern of Pt/CNT and Pt/Vulcan was refined on a cubic cell in the *Fm*3*m* space group using the FullProf Suite.[17] The Thomson–Cox– Hastings profile function was used to generate the line shape of the diffraction peaks.[18] The background was defined by linear interpolation between successive breakpoints in the pattern. The particle shape was simulated using the symmetrized spherical harmonics, which describe the dependence of the Voigt function on the integral width. The anisotropic strain was calculated from the Gaussian part of the profile, while the crystallite size anisotropy was given by the Lorentzian component of the total Voigt function. Large platinum particles were found in the synthesized samples. The D_{100}/D_{111} ratio for all of the synthesized catalysts is approximately the same. The shapes of the Pt nanoparticles were in the form of a truncated cube.[19]

Table 1 Characteristics of Pt/C catalysts.

Sample	X-ray diffraction				TEM
	a/Å	D_{111}/nm	D_{100}/nm	D_{100}/D_{111}	<*d*>/nm
Pt/CNT	3.9137	3.1	2.4	0.79	16.2
Pt/Vulcan	3.9195	7.6	6.0	0.78	10.4
JM	–	–	–	–	3.5

As shown in Table 1, the unit cell parameter of platinum nanoparticles for all samples is smaller than for bulk platinum owing to the size effect, which was reviewed and analyzed.[2]

It can be clearly seen [Figure 2(*a*)–(*c*)] that the introduction of CO into hydrogen results io a sharp decrease in the hydrogen oxidation current for all catalysts studied. A natural decrease in oxidation current is observed with increasing CO concentration. The highest residual oxidation current is observed for the Pt/CNT sample when hydrogen containing 10 ppm CO is used. The current for this catalyst is approximately five times higher than for Pt/Vulcan and JM samples [Figure 2(*d*)]. The Pt/Vulcan samples and the commercial JM catalyst have been completely poisoned by carbon monoxide during the test. The high surface oxidation rate of CO are associated with both platinum nanoparticles size and their agglomeration on the support surface and to the morphology of the carbon support.[21]

The electrotransport characteristics were studied in a three-electrode gas-liquid half-cell using impedance spectroscopy to identify the reasons for the significant tolerance of Pt/C electrocatalysts based on CNTs as support. The experimental results are shown in Figure 3(*a*)–(*c*) as the data points and the fitted curves according to the equivalent circuit are plotted as solid lines.

It is well known that the rate of an electrochemical reaction is determined by the reaction current. The reaction current is inversely proportional to the resistance of the electrochemical reaction:

$$i_0 = RT/nFR_f, \quad (1)$$

where i_0 is the exchange current, R – universal gas constant, T – absolute temperature; n – number of electrons, F – Faraday constant and R_f – Faraday resistance of an electrochemical reaction.

The higher the reaction rates of the hydrogen oxidation process on an electrocatalyst, the lower the resistance and the more resistant the catalyst is to poisoning. Therefore, the notion of process resistance is used to eliminate errors when comparing process rates. To estimate the rate of hydrogen oxidation, R_f measurements of the hydrogen process were carried out at high CO concentrations and corresponding potentials (see Figure 3).

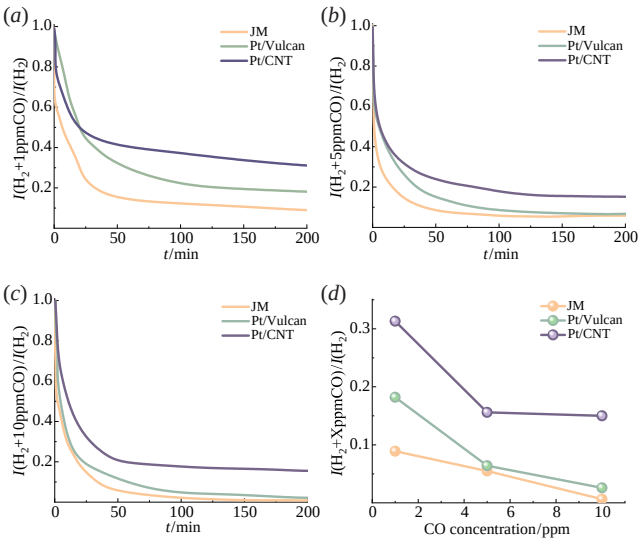

Figure 2 Relative oxidation current as a function of time for different CO concentrations: (*a*) 1 ppm, (*b*) 5 ppm, and (*c*) 10 ppm; (*d*) relative oxidation current as a function of CO concentration.

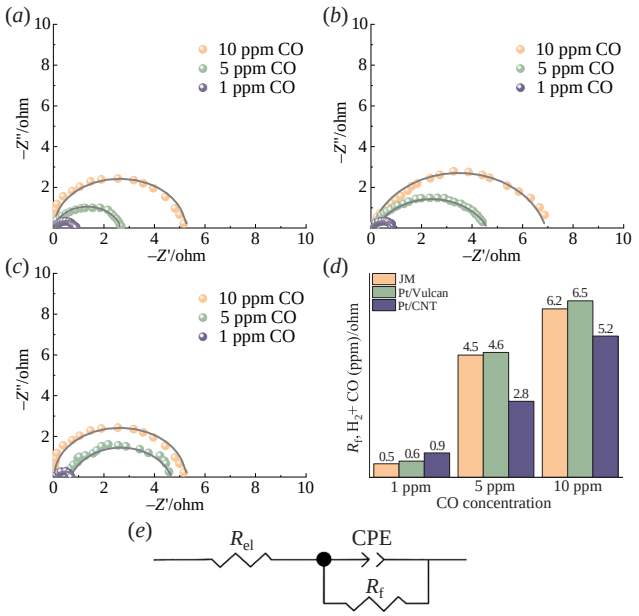

Figure 3 Impedance hodographs of catalyst samples: (*a*) JM, (*b*) Pt/Vulcan, (*c*) Pt/CNs. (*d*) Hydrogen electrooxidation reaction resistance (R_f). (*e*) Equivalent circuit for modelling electrochemical impedance of Pt/C catalysts in the presence of CO.

In the case of hydrogen–carbon monoxide mixtures, there are at least two components in the part of the hodograph corresponding to the electrode process. The first is a gross process involving carbon monoxide and the second is the process of electrooxidation of hydrogen. However, these processes are so close together that it is impossible to separate them. In addition, at CO concentrations above 1 ppm, the resistance of the carbon monoxide process becomes significantly higher than that of the hydrogen electrooxidation process, making it impossible to characterize the latter.

It should be also noted that R_f value for the Pt/CNT sample is 1.5 times higher than for Pt/Vulcan and 1.8 times higher than for the commercial JM sample in case of low concentration of CO (1 ppm). This indicates a lower CO tolerance of the Pt/CNT material compared to JM and Pt/Vulcan samples [Figure 3(*d*)]. However, at higher CO concentrations the opposite pattern was observed: the R_f parameter for Pt/CNT is lower by a factor of about 1.3–1.6 compared with the other catalysts. Such a difference could be due to the properties of the Pt/C materials themselves, in particular a higher degree of agglomeration of platinum nanoparticles on the surface of carbon nanotubes compared with carbon black-based catalysts, which can be clearly seen from the TEM results [Figure 1(*a*)–(*c*)]. An increase in the degree of agglomeration of Pt nanoparticles on the surface of the carbon support results in a decrease in the electrochemically active surface area of the platinum-containing catalyst, as shown by other researchers[22] and also in our work.[23] In addition, carbon materials are known to adsorb CO and they are used in the CO electrochemical detection.[24] Therefore, at relatively low concentrations of CO (1 ppm in this case) the increase in R_f could be due to non-uniform, incomplete filling of the Pt surface with carbon monoxide, along with CO crossover from the carbon support surface to the platinum. As the concentration of CO increases, the platinum surface becomes filled with CO, and the negative processes mentioned above no longer contribute to the resistance. However, Pt/CNT material posesses a higher CO tolerance compared with the other catalysts, especially at relatively high CO concentrations. This may be due to the presence of platinum agglomerates. The study conducted by Feliu *et al.*[25] on platinum CO oxidation processes revealed the impact of platinum nanoparticle agglomeration on CO oxidation kinetics. It was demonstrated that the overvoltage of the CO oxidation reaction on platinum agglomerates decreases owing to a distinct mechanism of interaction between CO and oxygen-containing species (intraparticle reaction and interparticle reaction).

The reaction resistance R_f was calculated by cyclic extrapolation (or arc extrapolation) from the impedance hodographs [see Figure (*a*)–(*c*)]. It can be clearly seen that as the CO concentration decreases, the resistance decreases (the corresponding semicircle decreases). The R_f values are shown in Figure 3(*d*). The resistance of the electrode process increases monotonically with increasing carbon monoxide concentration for all samples. In this case, the nature of the dependence of this resistance on the CO concentration is determined by the type and composition of the carbon support of the electrocatalyst. CNT-based electrocatalysts are more tolerant to carbon monoxide than the commercial analogue.

The impedance results were converted into equivalent electrical circuits [see Figure 3(*e*)] using the Equivalent Circuit program ZView (v. 3.5i). CPE (the constant phase element) was associated with the double layer capacitance, R_f the charge transfer resistance was associated with CO oxidation and R_{el} was associated with solution resistance.

In summary, catalysts synthesized under the action of AC pulsed current have a higher tolerance to CO poisoning. The synthesized catalysts are composed of quite coarse Pt particles of above 6–7 nm in size, for which the size-dependent CO_{ads} surface difusion, is less manifested.[26] In its turn, the Pt/CNT catalysts are much more stable than the Pt/Vulcan catalyst. These discrepancies could be attributed to variances in the kinetic or diffusion limited region of the samples. The differences in the kinetic or diffusion limited region can be explained not only by the properties of the active catalytic phase (Pt surface coverage, crystallite size number and number of active sites) but also by the properties of the carbon support (pore size distribution,[27] electrical conductivites[28] and carbon support morphology[29]). Variations in the properties of carbon support can cause structural discrepancies in the catalyst layer resulting in changes in its thickness. Consequently, there can be an impact on the current value in the diffusion limited region.

Thus, in this work we investigated the carbon monoxide poisoning resistance of various platinum-based catalysts. It has been shown that Pt/CNT catalysts based on carbon nanotubes as a support obtained under the influence of AC pulsed current have a higher tolerance to CO poisoning compared with Pt/Vulcan also prepared *via* pulse AC technique and commercial JM Pt/C catalyst which is widely used in PEMFC. The data obtained indicate that the use of reformed hydrogen as a fuel for PEMFC with the developed electrocatalysts is possible, although with a partial loss of power.

The work was carried out within the framework of the strategic project ‘Hydrogen Energy Systems’ of the Platov South-Russian State Polytechnic University (NPI) development program in the implementation of the strategic academic leadership program ‘Prioity-2030’.

Online Supplementary Materials

Supplementary data associated with this article can be found in the online version at doi: 10.1016/j.mencom.2024.04.042.

References

1 Y. Wang, D. F. Ruiz Diaz, K. S. Chen, Z. Wang and X. C. Adroher, *Mater. Today*, 2020, **32** 178.
2 M. A. Abdelkareem, K. Elsaid, T. Wilberforce, M. Kamil, E. T. Sayed and A. Olabi, *Sci. Total Environ.*, 2021, **752**, 141803.

3 H. L. Nguyen, J. Han, X. L. Nguyen, S. Yu, Y.-M. Goo and D. D. Le, *Energies*, 2021, **14**, 4048.
4 E. Yu. Safronova, O. V. Korchagin, V. A. Bogdanovskaya and A. B. Yaroslavtsev, *Mendeleev Commun.*, 2022, **32**, 224.
5 A. D. Manin, D. V. Golubenko, P. A. Yurova and A. B. Yaroslavtsev, *Mendeleev Commun.*, 2023, **33**, 365.
6 B. Shabani, M. Hafttananian, Sh. Khamani, A. Ramiar and A. A. Ranjbar, *J. Power Sources*, 2019, **427**, 21.
7 D. D. Papadias, J.-K. Peng and R. K. Ahluwalia, *Int. J. Hydrogen Energy*, 2021, **46**, 4169.
8 C. Acar and I. Dincer, *J. Cleaner Prod.*, 2019, **218**, 835.
9 R. Carapellucci and L. Giordano, *J. Power Sources*, 2020, **469**, 28391.
10 A. Midilli, H. Kucuk, M. E. Topal, U. Akbulut and I. Dincer, *Int. J. Hydrogen Energy*, 2021, **46**, 25385.
11 V. F. Valdés-López, T. Mason, P. R. Shearing and D. J. L. Brett, *Prog. Energy Combust. Sci.*, 2020, **79**, 100842.
12 E. G. Ciapina, S. F. Santos and E. R. Gonzalez, *J. Electroanal. Chem.*, 2018, **815**, 47.
13 A. B. Kuriganova, I. N. Leontyev, O. A. Maslova and N. V. Smirnova, *Mendeleev Commun.*, 2018, **28**, 444.
14 K. Novikova, A. Kuriganova, I. Leontyev, E. Gerasimova, O. Maslova, A. Rakhmatullin, N. Smirnova and Y. Dobrovolsky, *Electrocatalysis*, 2018, **9**, 22.
15 A. B. Kuriganova, I. N. Leontyev, M. V. Avramenko, N. A. Faddeev and N. V. Smirnova, *Mendeleev Commun.*, 2022, **32**, 308.
16 E. Antolini, *Appl. Catal., B*, 2009, **88**, 1.
17 J. Rodriguez-Carvajal, *Newsletter*, 2001, **26**, 12.
18 P. Thompson, D. Cox and J. B. Hastings, *J. Appl. Crystallogr.*, 1987, **20**, 79.
19 I. N. Leontyev, S. V. Belenov, V. E. Guterman, P. Haghi-Ashtiani, A. P. Shaganov and B. Dkhil, *J. Phys. Chem. C*, 2011, **115**, 5429.
20 I. N. Leontyev, A. B. Kuriganova, N. G. Leontyev, L. Hennet, A. Rakhmatullin, N. V. Smirnova and V. Dmitriev, *RSC Adv.*, 2014, **4**, 35959.
21 P. Urchaga, S. Baranton, C. Coutanceau and G. Jerkiewicz, *Langmuir*, 2012, **28**, 3658.
22 F. Maillard, S. Schreier, M. Hanzlik, E. R. Savinova, S. Weinkauf and U. Stimming, *Phys. Chem. Chem. Phys.*, 2005, **7**, 385.
23 A. Kuriganova, N. Faddeev, M. Gorshenkov, D. Kuznetsov, I. Leontyev and N. Smirnova, *Processes*, 2020, **8**, 947.
24 W. Zhao, D. W. H. Fam, Z. Yin, T. Sun, H. T. Tan, W. Liu, A. I. Y. Tok, Y. C. F. Boey, H. Zhang, H. H. Hng and Q. Yan, *Nanotechnol.*, 2012, **23**, 425502.
25 A. López-Cudero, J. Solla-Gullón, E. Herrero, A. Aldaz and J. M. Feliu, *J. Electroanal. Chem.*, 2010, **64**, 117.
26 F. Maillard, E. R. Savinova and U. Stimming, *J. Electroanal. Chem.*, 2007, **59**, 221.
27 G. A. Ferrero, K. Preuss, A. B. Fuertes, M. Sevilla and M.-M. Titirici, *J. Mater. Chem. A*, 2016, **4**, 2581.
28 G. Cognard, G. Ozouf, C. Beauger, I. Jiménez-Morales, S. Cavaliere, D. Jones, J. Rozière, M. Chatenet and F. Maillard, *Electrocatalysis*, 2017, **8**, 51.
29 M. A. Molina-García and N. V. Rees, *RSC Adv.*, 2016, **6**, 94669.

Received: 30th November 2023; Com. 23/7326